PARTICIPATION IN THE NEA/OECD MATiS-H BENCHMARK EXERCISE. STUDY OF SPACER GRIDS IN A ROD BUNDLE

C. Peña-Monferrer[a], S. Chiva[b,*], J. L. Muñoz-Cobo[a], E. Vela[c], F. Pelayo[c]

[a] *Institute for Energy Engineering, Universitat Politècnica de València. Camí de Vera, s/n, 46022 València, Spain*
[b] *Department of Mechanical Engineering and Construction, Universitat Jaume I. Campus del Riu Sec, 12080 Castelló de la Plana, Spain*
[c] *Consejo de Seguridad Nuclear. C/ Pedro Justo Dorado Dellmans 11, 28040 Madrid, Spain*

Abstract

Nuclear fuel bundles contain spacers essentially for mechanical stability and to influence the flow dynamic and heat transfer phenomena along the fuel rods. This work presents the analysis of the turbulence effects of a split-type and swirl-type spacer grid geometries on single-phase in a PWR (**P**ressurized **W**ater **R**eactor) rod bundle. Various **C**omputational **F**luid **D**ynamics (CFD) calculations have been performed and the results validated with the experiments of the OECD/NEA-KAERI Rod Bundle CFD Benchmark Exercise on Turbulent Mixing in a Rod Bundle with Spacers at the MATiS-H facility. The aim of this Benchmark is to provide validated CFD analysis tools providing a firm basis for quantifying the CHF Margin reliably for normal operation and operational transients conditions and allowing eventually the use of CMFD Codes for predicting DNB under accidental conditions [1]. Simulation of turbulent phenomena downstream of the spacer grid presents high complexity issues. A wide range of length scales are present increasing the difficulty of defining in detail the transient nature of turbulent flow. Calculations were performed with the commercial code ANSYS® CFX® and CFD modelling using **L**arge **E**ddy **S**imulation (LES) turbulence models by comparison with measurements to determine their suitability in the prediction of the turbulence phenomena. One of the most important aspects to be taken into account in order to properly simulate the flow downstream of the spacer grids is the use of a suitable turbulence model. Time-averaged values for all three velocity components, time-averaged RMS values of the fluctuating component of all three velocity components in several cross-planes downstream of the spacer grid and circulation data in a selected sub-channel are in good agreement with the measured data. These results could be of great value for future studies of spacer grid including heat transfer from the rods and as a basis of spacer grid simplifications.

Keywords: CFX, LES, Spacer Grid, MATiS-H, OECD, NEA, IBE-2

---

*Corresponding author
Email addresses: cmonfer@upv.es (C. Peña-Monferrer), schiva@emc.uji.es (S. Chiva), jlcobos@iqn.upv.es (J. L. Muñoz-Cobo), evb@csn.es (E. Vela), fpl@csn.es (F. Pelayo)

1. Introduction

In recent years the use of CFD numerical tools in nuclear engineering area has grown rapidly but still is not very mature in some specific areas. Hence the possibility of validate the complex physical phenomena happening in nuclear structures as spacer grids is highly appreciated.

The second International Benchmark Exercise on the turbulent mixing in a rod bundle is the OECD/NEA-KAERI Rod Bundle CFD Benchmark Exercise based on the MATiS-H (**M**easurament and **A**nalysis of **T**ubulent mixing **in** **S**ubchannels - **H**orizontal) experiments and provide a set of experimental data of time-averaged velocities and RMS of the fluctuating velocities from the end of the spacer grid to $10.0D_H$ downstream. The following data was released by KAERI on June 2012 for spacer grid with both split and swirl mixing vane:

- time-averaged values for all three velocity components
- time-averaged RMS values of the fluctuating components of all three velocity components
- the circulation in a selected sub-channel expressed as $\oiint \omega_z$ dxdy, where ω_z is the z-component of vorticity.

Results for spacer grids with split-swirl mixing vanes were presented in the blind benchmark and the results are analyzed in this paper. The relative quality of the CFD calculations submitted by all the participants was compared in [1] with some ranked results.

2. Benchmark test description

The MATiS-H located at the Korea Atomic Energy Research Institute (KAERI), Daejeon, Korea, is illustrated in Fig. 1. The test rig consists of a channel of 170 mm side length and 4.670 mm long and a 5x5 rod bundle of 25.4 mm of rod diameter and 3.863 mm long [2]. The hydraulic diameter of the channel (D_H) is 24.27 mm. The spacer grid with mixing vanes, 2.6 times larger than the size of PWR fuel bundles, is located inside the channel for generating lateral turbulent mixing in sub-channels.

The measurement section is fixed at a position 10 mm upstream of the end of the rod bundle. The spacer grid can be moved axially to increase the downstream distance (Z_D in Fig. 1) of the measurement section. The 2nd flow straightener allows expected identical inlet flow conditions upstream of the spacer. The distance L_{FD} is set at 100 DH to have a fully developed flow profile at the inlet to the spacer grid.

The experiments have been made for two different types of mixing vanes: split type (Fig. 2a) and swirl type (Fig. 2b). In both cases axial and lateral velocities were measured and turbulent intensities and vortices in sub-channels were then evaluated from the velocity measurements.

3. CFD simulation setup

In this section the CFD simulation setup developed for investigating spacer grid effects in MATiS-H facility is presented. The simulations described here represent the participation in the

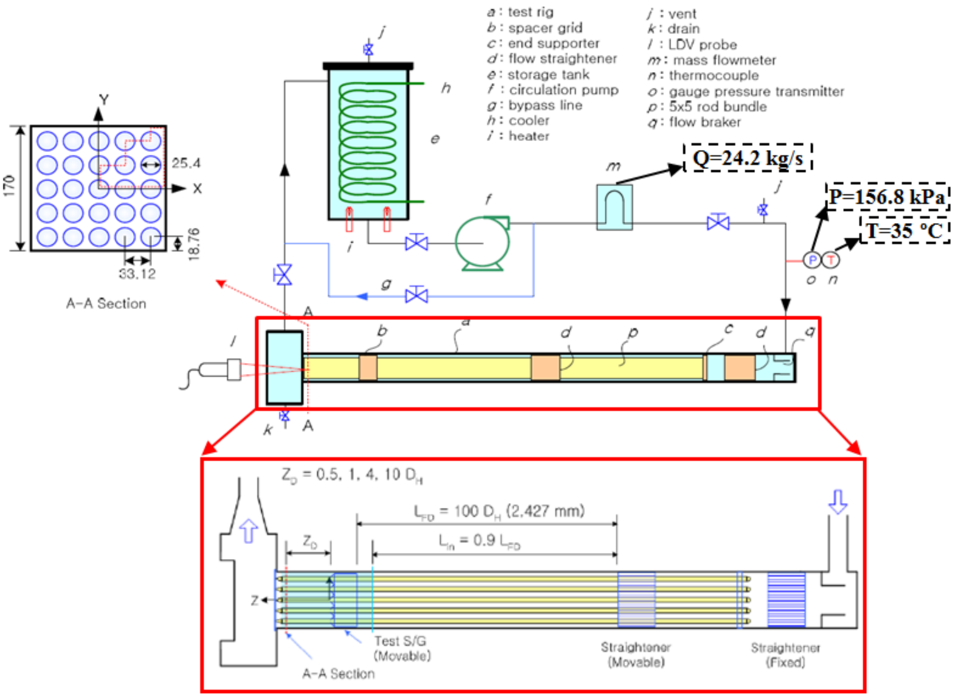

Figure 1: Schematic diagram of the MATiS-H test facility and location of velocity measurements [1]

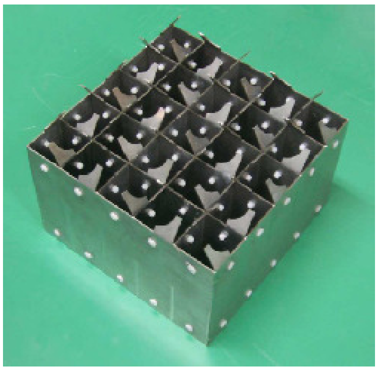

(a) Split-type of mixing vanes

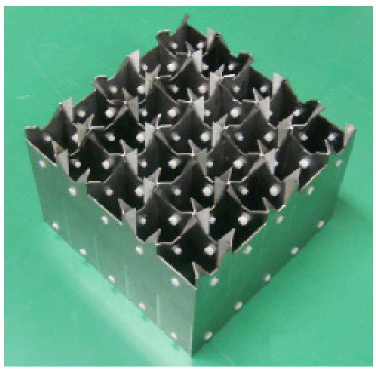

(b) Swirl-type of mixing vanes

Figure 2: Types of spacer grids tested in MATiS-H [1]

concerned blind Benchmark. A brief description of geometry modeling, meshing and CFD setup of the physical models will be provided.

The test rig of the benchmark has a relatively large test section. Consequently a modeled simulation of the whole experiment seems unreasonable so it is required to reduce the computational domain and define appropriate boundary conditions. Hence we have incorporated a set of measures and simplifications to achieve a feasible simulation. The geometry of the spacer grids provided by KAERI was included in the rest of the geometric model based on the geometry specifications. The CFD simulation are realized with the commercial code ANSYS® CFX® 13.0

3.1. Computational domains

The model has been divided in two domains in order to optimize the meshing and the physical modeling depending on the flow characteristics (Fig. 3). One domain is a bare rod bundle of 90 D_H starting at the end of the second flow straightener marked as "d" in Fig. 1. A constant mass flow rate is used as an inlet boundary condition and the uniformity of the flow in the inlet must be guaranteed by the flow straightener immediately upstream located in the experiment. For convenience, the domain considering the spacer grids has an inlet boundary condition defined at 10 D_H upstream of the beginning of the spacer grid.

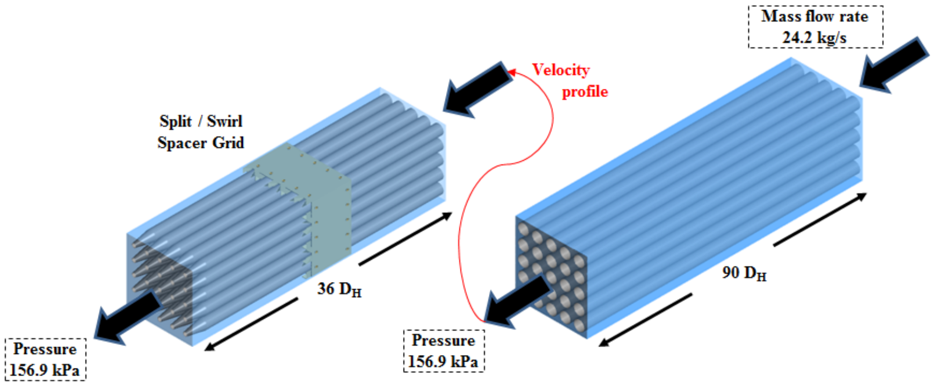

Figure 3: Inlet and outlet boundary conditions for the bare rod bundle and the model with spacer grid

3.2. Mesh generation

The mesh was created using the ANSYS® ICEM CFD™13.0 software obtaining a mesh as uniform as possible and at the optimum size to cover the variations of fluid characteristics. Due to the characteristics of the simulation, a large number of nodes should be considered. An agreement between the number of nodes (meeting the Best Practice Guidelines [3]), which affects the margin of error, and the computational resources required, has to be found.

The mesh procedure was generated in a first step with the Octree mesh method. Next, the specified prism elements in every region were created in successive layers away from the wall. A total of 10 layers with a exponential growth rate between them it is applied, due to the narrow distance between some spacer grid walls, the number of layers must be adapted to avoid bad quality of the elements and collisions between layers. The longitudinal mesh size was controlled with a previous axial scaling in two different areas, upstream and downstream including spacer grid.

A computational mesh grid of around 26 millions of elements are resulted with a transverse mesh size of 1.8 mm. The mean y^+ obtained is 1.08.

3.3. Boundary conditions

The outlet boundary condition is always established as a constant pressure. The pressure value provided by KAERI with a gauge pressure transmitter is located at the inlet of the test rig. In order to know pressure in the location desired it would be needed to simulate the whole test rig but it would be required excessive computational time, resource time and design time.

The incompressible flow is maintained isotherm (35 C). Since the pressure drop of the computational domain considered (see Fig. 3) is around 3000 Pa the change of density and viscosity are well below a change of 0.001% and then one consider constant properties for the water and neglects the effect of the pressure drop caused by the flow straighteners, rod bundle supports, flow breaker in order to save valuable computational time. For this reason we will consider an outlet boundary conditions matching the reference pressure, 156.9 kPa, without loss of accuracy in the simulation.

The boundary conditions in the wall are established as "automatic near-wall treatment" implemented in CFX, which automatically switches from wall functions to a low- Reynolds near wall formulation as the mesh is refined.

3.4. Turbulence modelling

The turbulence model selected for the preliminary simulations to solve the inlet flow profile was the Shear Stress Transport (SST) model because of the simplicity of the flow in this area. A previous simulation with RANS turbulence model was required as an initialization values for the LES simulations. This turbulence model was the Shear Stress Transport (SST) model and after getting convergence, we started using the LES model with the Smagorinsky subgrid-scale model.

4. Results and discussion

A computational time of 345 hours to reach 1.25 s of transient time was required in a linux workstation Intel Xeon E5645 @ 2.40 GHz with 48 GB RAM. The timestep selected permits a resulting RMS courant number of 1.12.

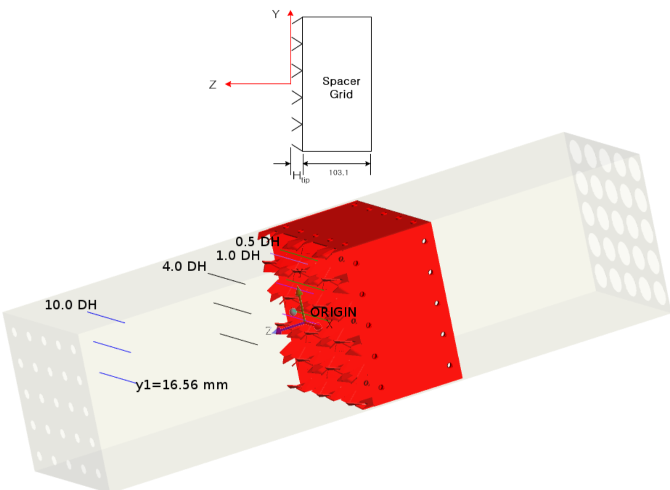

Figure 4: Measurement lines at from the specified origin coordinate system

The comparison of the CFD results with the measured data at the y1 elevation (see Fig. 4) for mean and RMS velocity values in three measurements planes at 1.0 D_H, 4.0 D_H and 10.0 D_H for the three components u, v and w are shown in Fig. 5. The x axis represents the position from the center of the channel to the wall and is normalized with the pitch distance. Mean and RMS velocities are normalized with the W_{bulk} velocity.

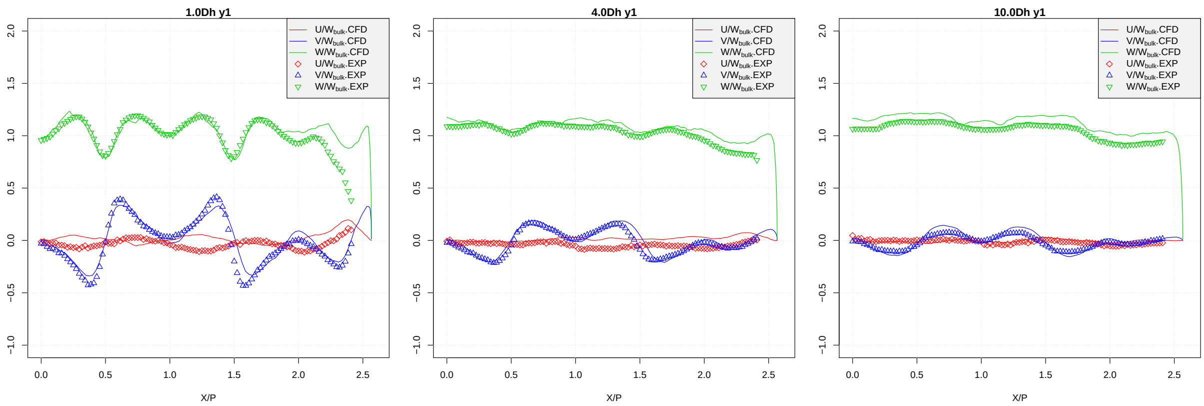

(a) Mean velocities at 1.0 D_H (b) Mean velocities at 4.0 D_H (c) Mean velocities at 10.0 D_H

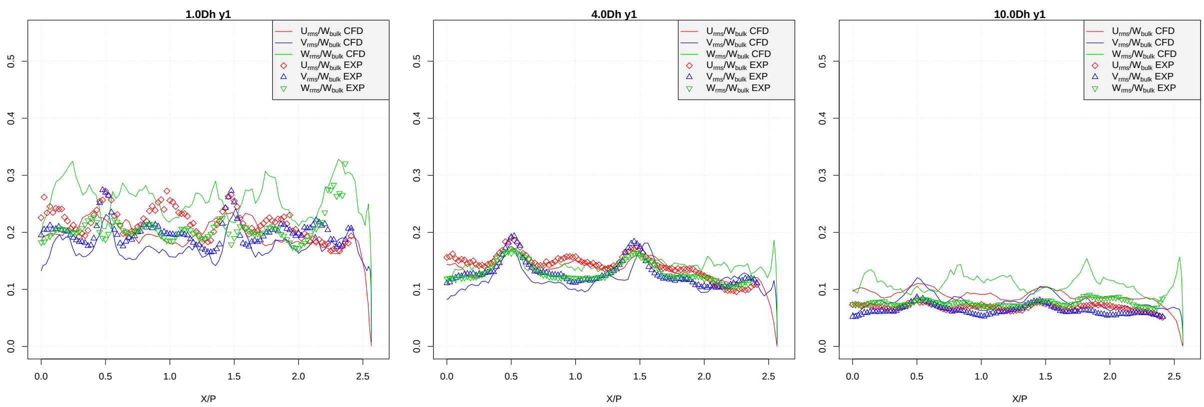

(d) RMS fluc. velocitiesy at 1.0 D_H (e) RMS fluc. velocities at 4.0 D_H (f) RMS fluc. velocities at 10.0 D_H

Figure 5: Mean and RMS velocity components

The evolution of the mean z-component vorticity along the downstream of the spacer is shown for the four different measurement planes (z=0.5D_H, 1.0D_H, 4.0D_H and 10.0D_H) in Fig. 6.

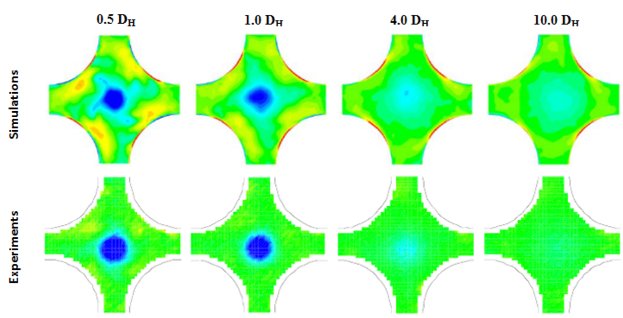

Figure 6: Vorticity contours from experimental (down) and simulations (up) results at the four measurament planes

The results obtained in our simulations show a good capability to capture the turbulence phenomena and the procedure of production of turbulence and dissipation. The small error between the CFD results and the experimental data may result from simplifications or probably the need of a local refinement in the mesh and the global mesh size in the streamwise direction. The assumption of an small error was accepted in benefit of the computational resources required. Furthermore the decay of the turbulence downstream of the vanes seems in good agreement.

In Fig. 7a and Fig. 7b it is possible to see the dissipation process in the four different measuring planes. Values of time-averaged velocity and time-averaged RMS values of the fluctuating velocity in the z-axial component:

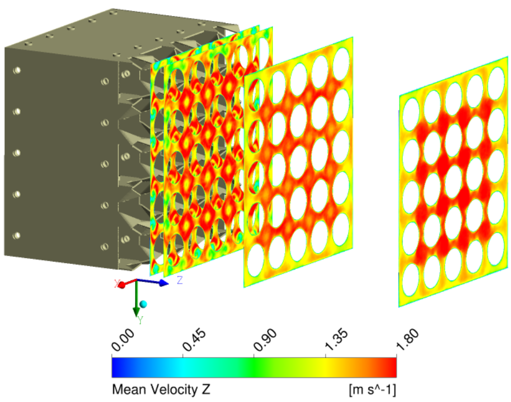

(a) Mean velocity w-component

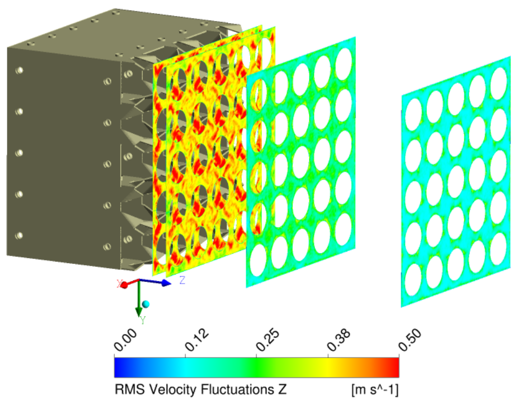

(b) RMS fluctuation velocity w-component

Figure 7: Mean and RMS velocity at the four measurement planes

As additional information, quantitative images are extracted of the CFD results in order to see the flow behavior produced by the spacer grids. Streamlines representing the flow leaving the spacer around only one rod are illustrated in Fig 8.

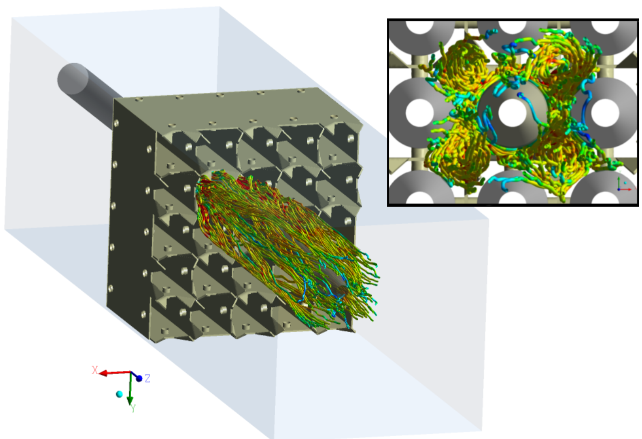

Figure 8: Streamline of flow leaving the spacer around one rod

5. Conclusions

A CFD model for a rod bundle with a spacer grid has been validated with experimental data. The results obtained were presented to the blind benchmark and selected as Best Estimation Case of the LES turbulence model submitted and the results related with swirl mixing vane obtained a ranked results of 3^{rd} at 1.0 D_H and 1^{st} at 4.0 D_H downstream of the vanes (only ranked results at 1.0 D_H and 4.0 D_H were provided at the time of the publication of this paper) [1]. The mesh size of the fifteen results submitted to the blind benchmark are in a range of 3 (only sub-channel simulation) to 110 millions of elements. The mesh of our participation is the fifth coarser mesh.

Future work will include a constant heat transfer from the rods to analyze the influence of the spacer grid in the temperature profiles in the sub-channels.

Furthermore, as a part of the ongoing research to define a methodology for CFD fuel assemblies simulations to consider spacer grid effects as pressure drop and also turbulence enhancement without model them, the validation of this model will be useful as a basis to verify it.

Acknowledgements

The authors sincerely thank the CSN - Consejo de Seguridad Nuclear (Spanish Nuclear Safety Council) and the “Plan Nacional de I+D+i” Project EXPERTISER ENE2010-21368-C02-01 and ENE2010-21368-C02-02 for funding the project.

References

[1] J. R. Lee, J. Kim, C.-H. Song, Synthesis of the OECD/NEA-KAERI rod bundle CFD benchmark exercise, in: Proc. CFD4NRS-4, OECD/NEA & IAEA Workshop, Daejon, Korea.

[2] S.-K. CHANG, S. KIM, C.-H. SONG, OECD/NEA-KAERI Rod Bundle CFD Benchmark Exercise Test, in: Proc. CFD4NRS-4, OECD/NEA & IAEA Workshop, Daejon, Korea.

[3] Nuclear Energy Agency - Committee On The Safety Of Nuclear Installations, Best practice guidelines for the use of CFD in nuclear reactor safety applications , Technical Report NEA/CSNI.